RSC Advances

PAPER

View Article Online
View Journal | View Issue

Cite this: *RSC Adv.*, 2021, **11**, 39907

The kinetic model of cyclohexene–air combustion over a wide temperature range†

Hongbiao Lu,[ab] Wenhui Kong,[ab] Changhua Zhang,[bc] Jingbo Wang *[ab] and Xiangyuan Li [ab]

Cyclohexene is an important intermediate during the combustion process of hydrocarbon and oxygenated fuels. In view of the lack of study on the combustion of cyclohexene in air, an experimental and modeling study is performed to investigate the chemistry of cyclohexene–air mixtures under a wide temperature range. The shock tube experiments are conducted at pressures of 2 and 10 atm with equivalence ratios of 0.5, 1.0 and 2.0 to determine the ignition delay times. The ignition data under 10 atm cover a wide temperature range varying from a low temperature of 770 K to a high temperature of 1222 K. No typical negative-temperature-coefficient is observed, but the ignition at low temperatures is shorter than the extrapolation at high temperatures. A detailed kinetic model of cyclohexene oxidation is proposed based on the low temperature mechanism of 1,3-cyclohexadiene and the existing high temperature mechanism of cyclohexene. The developed model reproduces the ignition delay times in air well, but it over predicts the ignition delays in argon conditions at higher temperatures. Sensitivity analyses under different temperatures and equivalence ratios are carried out to identify the key reactions affecting ignition. The reactions of H + O_2 = O + OH and hydrogen abstraction reaction of cyclohexene with oxygen (CYHEXEN + O_2 = CYHEXEN-3J + HO_2) explain the change of ignition delay time of cyclohexene with equivalence ratios. Flux analysis gives the change of main reaction pathways under wide temperatures and different pressures. The retro-Diels–Alder reaction as the most important consumption channel of cyclohexene at the pressure of 2 atm and temperature of 1350 K is greatly suppressed when the pressure is increased to 10 atm, while the hydrogen abstraction reaction becomes the main consumption channel of cyclohexene at the high pressure. The proposed kinetic model for cyclohexene oxidation can be used to develop models of hydrocarbon and oxygenated fuels.

Received 23rd September 2021
Accepted 2nd December 2021

DOI: 10.1039/d1ra07122j

rsc.li/rsc-advances

1. Introduction

Alkenes is not only an important intermediate in the combustion of hydrocarbon fuels[1] and oxygenated fuels,[2,3] which has a significant impact on the combustion characteristics of fuels, but also can be used as an surrogate component of real fuels[4,5] to study their combustion process. For many years, the studies of alkenes have focused on the lighter ones such as ethylene,[6–10] propene,[1,11–13] butene,[14–16] pentene,[4,17,18] acyclic C6 alkenes[19–21] and cyclo-C5 alkenes.[22,23] Cyclohexene is an important intermediate in the combustion process of cycloalkanes, such as cyclohexane and ethylcyclohexane,[24,25] which mainly comes from the β-scissions of free radicals on the ring. The study of combustion mechanism of cyclohexene will be beneficial to the study of combustion kinetics of cycloalkanes. It has long been reported that cyclohexene participates in the formation of benzene,[26,27] which is the first aromatic ring in the formation of polycyclic aromatic hydrocarbons (PAHs). Therefore, the study of cyclohexene combustion can help us better understand soot formation during the combustion of cyclic fuel.

The experimental data for cyclohexene oxidation, available from the literature up to now, are summarized in Table 1, which mainly focus on the measurement of ignition delay time under argon (Ar) dilution conditions. The corresponding kinetic models are listed in Table 2. Lemaire *et al.*[28] measured the ignition delays for cyclohexene–O_2–inert (N_2/Ar/CO_2) mixtures in rapid compression machine (RCM) at 600–900 K, 7–14 atm and equivalence ratio of 1. They concluded that cyclohexene has a narrow negative temperature coefficient (NTC) region near 750 K, spanning about 20 K. Dayma *et al.*[29] reported the ignition delay times for cyclohexene/O_2/Ar mixtures at 7.7–9.1 atm, equivalence ratios of 0.5, 1 and 2, and temperatures between 1050 K and 1520 K. The experimental results show that the ignition delay time varies with equivalence ratio and fuel

[a]College of Chemical Engineering, Sichuan University, Chengdu 610065, China. E-mail: wangjingbo@scu.edu.cn
[b]Engineering Research Center of Combustion and Cooling for Aerospace Power, Ministry of Education, Sichuan University, Chengdu 610065, China
[c]Institute of Atomic and Molecular Physics, Sichuan University, Chengdu 610065, China

† Electronic supplementary information (ESI) available. See DOI: 10.1039/d1ra07122j

Table 1 The experimental data for cyclohexene oxidation on ignition delay times

Reactor	Mixture	T (K)	p (atm)	Φ	Dilution (%)	Ref.
RCM	Cyclohexene/O_2/Ar/N_2/CO_2	600–900	7–14	1	Air	Lemaire *et al.*[28]
ST	Cyclohexene/O_2/Ar	1050–1520	8.5	0.5–2	64–90.5%	Dayma *et al.*[29]
ST	Cyclohexene/O_2/Ar	1310–1540	6.4	1	95.25%	Giarracca *et al.*[30]
ST	Cyclohexene/O_2/N_2	770–1356	2–10	0.5–2	Air	This work

concentration. Giarracca *et al.*[30] studied the ignition delay time of four C6 cyclic hydrocarbon fuels (cyclohexane, cyclohexene, 1,3-cyclohexadiene, and 1,4-cyclohexadiene). The shock tube (ST) experiments were performed under Ar dilution, the ignition temperature over 1200 K, and mean pressure of 6 atm. Experimental results and the previous literature data[29,31] show that the reactivity of the four fuels when the temperature is higher than 1400 K is in the order of cyclohexene > 1,4-cyclohexadiene > cyclohexane > benzene ≈ 1,3-cyclohexadiene.

Regarding chemical kinetic models simulating cyclohexene oxidation, Table 2 shows the mechanism models of cyclohexene oxidation currently available and their scope of application.

Lemaire *et al.*[32] established a kinetic model for the low temperature oxidation of cyclohexene involving 136 species and 1064 reactions. The simulation results matched their earlier measurements in RCM.[28] The addition reaction of cyclohexene and HO_2 to the formation of OH plays a significant role on the ignition of cyclohexene by mechanism analysis. However, there is unavailable to get detailed kinetic and thermodynamic data from their work. Dayma *et al.*[29] established a high temperature oxidation model of cyclohexene based on the C0–C6 reactions of unsaturated soot precursors, including 123 species and 843 reactions. This kinetic mechanism can reproduce the experimental data of other working conditions except for the equivalence ratio of 0.5. A kinetic model of the high temperature ignition of the four cyclo-C6 fuels on shock wave measurements was constructed by Giarracca *et al.*[30] The mechanism is constructed based on the mechanism of Dayma *et al.*[29] combined with their own theoretical calculations. The model generally reproduces the reactively trend of the four fuels, but there is a large deviation in the simulation of cyclohexene. In addition, as an intermediate of many hydrocarbon fuels, the reactions related to cyclohexene occasionally occurs in the mechanism of hydrocarbon fuels, such as cyclohexane,[33] methylcyclohexane,[34] decalin,[35] and JetSurF 2.0 mechanism.[36] However, these mechanisms cannot reproduce the existing ignition experimental data well due to their incomplete reaction network for cyclohexene. Besides, Schönborn *et al.*[37] constructed a low temperature oxidation model of 1,3-cyclohexadiene including 421 species and 1791 reactions. Their mechanism includes the low temperature oxidation pathway of cyclohexene, that is, the main chain branching reaction pathway ($\dot{R} + O_2 \rightarrow R\dot{O}_2 \rightarrow \dot{Q}OOH \rightarrow \dot{O}_2QOOH \rightarrow 2OH$ + stable species) and the side chain reaction pathway (synergistic elimination of $R\dot{O}_2$ radicals, formation of cyclic ethers, and β bond breaking of QOOH radicals, *etc.*).[38,39] Hence, this mechanism can be used as the basis for the improvement of cyclohexene mechanism.

As can be seen from the above description of cyclohexene oxidation, there is a lack of ignition data under air conditions, especially at low temperature. In the present work, the combustion mechanism for cyclohexene–air mixture is elucidated through experimental and modeling studies. Systematic experiments are performed to determine the ignition delay time for cyclohexene–air mixtures at a wide range of temperatures from 770–1360 K, pressures from 2 atm to 10 atm, and equivalence ratios of 0.5–2. A detailed kinetic model is developed based on the mechanism of 1,3-cyclohexadiene,[37] and verified with the experimental data of present work and other literature values. Sensitivity analysis and flux analysis are carried out to point out the important reaction channels that affect the ignition. The developed model is helpful for improving the combustion model of cyclic fuels.

2. Experimental method

The ignition delay time of cyclohexene was measured in a shock tube and the obtained data are listed in Table S1 of ESI.† Due to the lack of experimental data for cyclohexene/air in the literature, the reliability of present data cannot be explained by comparison. However, the shock tube device has been successfully applied to our previous low-to-high temperature ignition research work.[40–44] Among them, Yang *et al.* got the ignition delays of ethylene/air in shock tube spanned a wide temperature range from 721 K to 1320 K.[43] The experiments on stoichiometric *n*-heptane/air mixtures were carried out at pressures of 2 and 10 atm, and temperatures of 700–1400 K.[44] The

Table 2 The summary of mechanisms of cyclohexene

Model	Temperature range	No. of species	No. of reactions
Lemaire *et al.*[32]	Low temperature	136	1064
Dayma *et al.*[29]	High temperature	123	843
Giarracca *et al.*[30]	High temperature	367	2318
Developed model in this work	Wide temperature range	443	1883

ignition data has been compared with the experimental results of Ciezki *et al.*[45] and Heufer *et al.*[46] to prove the reliability of the experimental facility. The experimental details have been introduced in the previous literature, thus only a brief description is given in this section. The inner diameter of the shock tube is 10 cm, and the driver section (6 m) and the driven section (5 m) are separated by a 3 cm double diaphragm section. Different reflected shock pressures of 1–10 atm are generated by blasting polycarbonate diaphragms of different thicknesses. In order to prevent condensation of the fuel, the driven section was wrapped with electric heating ring. Six independent current circuits were used to provide a uniform temperature distribution along the tube length. The shock tube was evacuated to $\sim 10^{-2}$ Torr with a vacuum pump before each experiment. The mixture of cyclohexene and synthetic air (21% O_2 and 79% N_2) was pre-vaporized in a 40 L stainless steel mixing tank and mixed for more than 2 h. The incident shock velocities were measured by four piezoelectric pressure transducers (PCB 113B) over the last 75 cm of the test section. The pressure signals were collected by a digital oscilloscope (Tektronix DPO5054). The ignition temperature T and pressure p of the reflected shock wave were derived from the measured initial temperature and pressure of the driven section, the incident wave velocity and the thermodynamic characteristics of the reactant mixture by using the ideal one-dimensional wave equation. On the last PCB section 15 mm away from the shock tube end wall, the light emission was exported using a quartz optical fiber. Two monochromatic tubes coupled with a photomultiplier tube were set at 431 nm to detect the chemiluminescence of CH*. The definition of ignition delay time is the time interval between the arrival of the reflected shock wave represented by the sharp rise of pressure signal and the ignition start determined by the sudden increase of the CH* signal, as shown in Fig. 1. Due to the non-ideal boundary layer effect and non-ideal fluid dynamics, it will cause a significant release of ignition energy, which will cause the pressure before ignition to rise,[47,48]

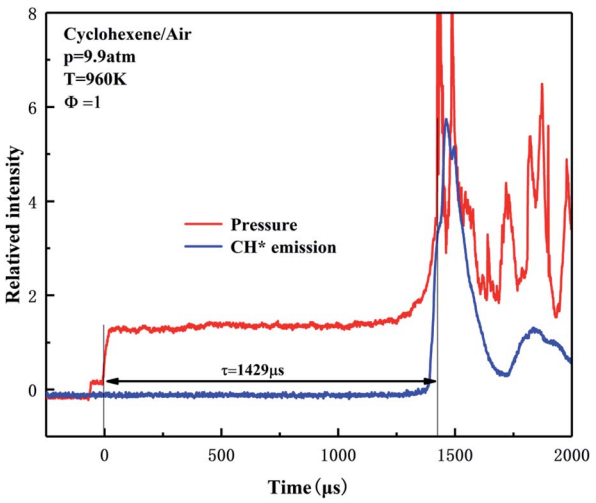

Fig. 1 Examples of ignition delay time definition for cyclohexene–air mixtures. The red line and blue line show the change curves of pressure and CH* signal, respectively.

and a smaller ignition delay time will be obtained under low temperature conditions. This issue has been clarified in previous studies,[49–51] so the CONP-VITM method (*i.e.*, constant enthalpy and pressure modeling combining with volume as a function of time) is often employed for shock tube modeling research.[41,43,52] In this work, it can be seen from Fig. 1 that there is a slight pressure rise caused by the interaction between the reflected shock wave and the boundary layer before the main ignition. And, the variation in the pressure is determined to be in the range of $(dp/dt)/(1/p_0) = 0$–5% ms^{-1}. The overall uncertainty of the measured ignition time is estimated to be within ±20%, including the uncertainty of the reflected pressure and temperature, the composition of the reactant mixture, and the uncertainty of the ignition delay determined by the pressure and CH* signal changes.

3. Kinetic model development

Cyclohexene has a cyclic structure with a C=C double bond. The complexity of the structure increases the difficulty of modeling its combustion kinetics.[32] The mechanism of 1,3-cyclohexadiene[37] is chosen as the base to construct the mechanism of cyclohexene in the present work, due to its detailed low temperature oxidation channels. The C3–C4 reactions of this mechanism come from the work of Fournet R. *et al.*[53] And the C5–C6 part about cyclopentadiene and benzene was made by B. Sirjean *et al.*[54] However, this mechanism lacks high temperature reaction pathways for cyclohexene. According to the work of Dayma *et al.*[29] and their mechanism analysis results, the high temperature oxidation channels of cyclohexene are added into the mechanism of 1,3-cyclohexadiene in order to build a combustion mechanism over a wide temperature range. The added representative reaction types are explained in the following section. For clarity, the names and molecular structures of the species involved in the developed model are given in Table S2 of ESI.†

Table 3 lists the added high temperature reaction types of cyclohexene and the corresponding representative reactions. The single molecular decomposition reaction of cyclohexene contains retro-Diels–Alder reaction R1 to form ethylene (C_2H_4) and 1,3-butadiene (C_4H_6), dehydrogenation reaction R2 to 1,3-cyclohexadiene (CYHEXDN13) and hydrogen (H_2), and C–H bond breaking reaction R3 and R4 to generate cyclohexenyl radicals (CYHEXEN-3J, CYHEXEN-4J). The second type of reaction added is the hydrogen abstraction (H-abstraction) reaction of cyclohexene, which generates two different cyclohexene radicals (CYHEXEN-3J and CYHEXEN-4J) by consuming 8 different radicals and molecules (H, O, OH, O_2, HO_2, CH_3, *etc.*). In order to make the simulation results of the model more consistent with the experimental data, the pre-exponential factor of reaction R5, that is the hydrogen atom abstracting hydrogen from the allylic position of cyclohexene, is multiplied by 3. The original rate constant of this reaction was estimated by analogies with uncertainties.[29] It is acceptable to adjust the kinetic parameter within a small range. The improvement of the simulation results after this parameter modification is shown in Fig. S1.† The third type of reaction added is the addition

Table 3 The added high temperature reaction types of cyclohexene and the representative reactions. The rate constants of high temperature reactions are derived from the work of Dayma[29] in the modified Arrhenius formula ($k = AT^n \exp(-E_a/RT)$). Units in mol, cm^{-3}, s, cal

Reaction types	No.	Representative reactions	A	n	E_a	Ref.
Decomposition	R1	CYHEXEN = C_2H_4 + C_4H_6	1.50×10^{15}	0	6.69×10^4	29
	R2	CYHEXEN = CYHEXDN13 + H_2	5.00×10^{13}	0	6.17×10^4	29
	R3	CYHEXEN = CYHEXEN-4J + H	5.00×10^{15}	0	9.89×10^4	29
	R4	CYHEXEN = CYHEXEN-3J + H	1.20×10^{15}	0	8.32×10^4	29
H-abstraction	R5 [a]	CYHEXEN + H = CYHEXEN-3J + H_2	3.30×10^5	2.50	-1.90×10^3	29
	R6	CYHEXEN + OH = CYHEXEN-3J + H_2O	6.00×10^6	2.00	-5.20×10^2	29
	R7	CYHEXEN + HO_2 = CYHEXEN-3J + H_2O_2	6.00×10^{12}	0	1.35×10^4	29
Addition	R8	CYHEXEN + OH ⇒ C_2H_3CHOZ + $R_{19}C_3H_7$	5.00×10^{12}	0	0	35
	R9	CYHEXEN + HO_2 ⇒ $cC_6H_{10}O$ + OH	4.53×10^3	2.84	1.45×10^4	55
	R10	CYHEXEN + H = cC6H11	2.60×10^{13}	0	1.56×10^3	29
Sub-mechanism of cyclohexane	R11	cC_6H_{11} + O_2 = $cC_6H_{10}O_2H$-2	6.95×10^{13}	0	1.21×10^4	36
	R12	$cC_6H_{10}O_2H$-2 ⇒ OH + B_2CO + $C_5H_{10}Z$	2.45×10^{12}	0	1.81×10^4	36
	R13	$cC_6H_{10}O$ + OH ⇒ H_2O + RC_6H_9OK	2.20×10^6	2.00	-1.87×10^3	57

[a] Modified based on ref. 29.

reaction of cyclohexene with H, O, OH, HO_2 and CH_3. The subsequent oxidation and bond breaking reactions of the addition products are also added, such as R8 and R9. The rate constant of R8 is derived from the decalin mechanism constructed by Dagaut *et al.*[35] Reaction R9 is considered to be a chemical activation reaction, and its pressure-dependent rate constant is calculated by the multi-well master equation of Zádor *et al.*[55] Moreover, the addition products of cyclohexene such as cyclohexyl (cC_6H_{11}), cyclohexane hydroperoxide radical ($cC_6H_{10}O_2H$-2) and cyclic ether ($cC_6H_{10}O$) are the intermediates in the low temperature oxidation reaction of cyclohexane, so the related low temperature reactions of cyclohexane in JetSurF 2.0 (ref. 36) have also been added to the developed model. Finally, the developed mechanism contains 443 species and 1883 reactions. The complete kinetic model and the associated thermodynamic data are provided in the SI. Thermodynamic data for the species are derived from existing literature[36,56–59] or calculated by the RMG program with the group additivity method.[60]

4. Model validation and analyses

4.1 Ignition delay time validations

The ignition delay time reflects the combustion characteristic of fuel, which is an important indicator to verify whether the combustion mechanism of hydrocarbon fuel is reasonable. In present work, the simulations of ignition delay time were performed in a zero-dimensional closed homogeneous reactor[61] with the Chemkin-Pro package.[62] Under the high temperature conditions, within a relatively short period of ignition time, there is almost no difference between using the traditional CONV (constant internal energy and volume) and using the CONP-VITM method to predict the ignition delay time. However, due to the influence of equipment effect, the CONP-VITM method using a pressure rise of 3% ms^{-1} is performed to obtain the ignition time under low temperature conditions.

Fig. 2 depicts the ignition delay times of cyclohexene–air mixtures at pressures of 2 and 10 atm, equivalence ratios of 0.5, 1, and 2. The ignition data under 10 atm span a wide temperature range varying from a low temperature of 770 K to a high temperature of 1222 K. For the ignition at high temperatures, as can be seen from Fig. 2a, there is a crossover between the ignition delay times of the three different equivalence ratio mixtures, which is consistent with the results of other alkenes.[43,63] The trend means that the reactivity of the fuel-lean mixture begins to exceed that of the fuel-rich mixture. The main reason can be obtained from the sensitivity analysis at different equivalence ratios of cyclohexene–air mixtures. As shown in Fig. 5, at high temperature of 1200 K, chain branching reactions such as H + O_2 = O + OH play a leading role in promoting fuel ignition. Its sensitivity coefficient increases with the equivalence ratio decreasing. The relatively high oxygen concentration at lower equivalence ratio improves the reactivity of the fuel and reduces the ignition time. No typical NTC region is observed in Fig. 2b, but the ignition delay time at low temperature is much shorter than that obtained by high temperature extrapolation. Lemaire *et al.*[28] found that cyclohexene has a weak NTC region between 730–750 K in RCM. Moreover, Fig. 2b shows that cyclohexene ignites faster at high pressure for the same equivalence ratio. This probably because the increase in pressure leads to an increase in the absolute concentration of reactants, which increases the reactivity of the system. In addition, the rate constant of some pressure-related reactions may rise sharply due to the increase of pressure,[55,64,65] which leads to an increase in the reactivity of the system. Although the simulated value is slightly lower than the experimental data, the maximum deviation is about 25%. In general, the developed model predicts the ignition delay time of cyclohexene–air mixture at various pressures, temperatures and equivalence ratios well.

Based on the existing experimental data of ignition delay time of Giarracca *et al.*[30] and Dayma *et al.*,[29] the developed model is verified for the different compositions of cyclohexene/O_2/Ar mixtures. As shown in Fig. 3a, the ignition delay time is

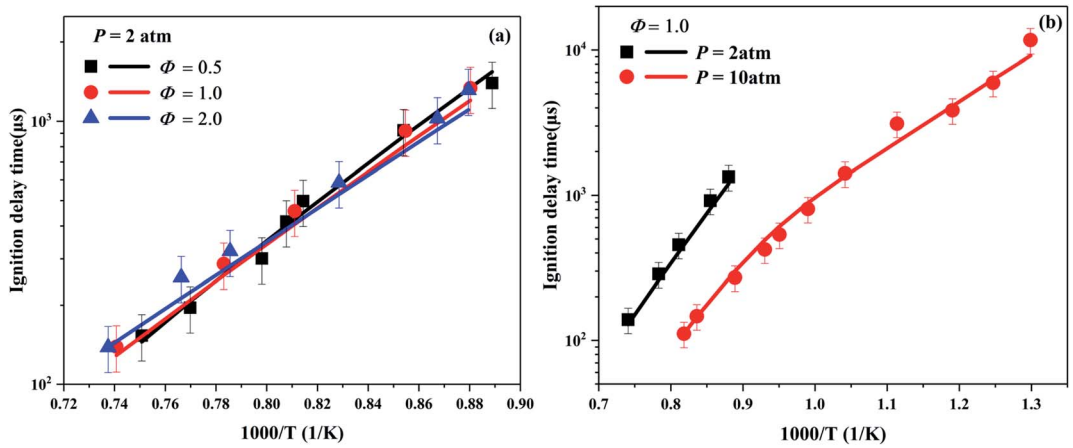

Fig. 2 The ignition delay time of cyclohexene–air mixtures. (a) The effect of equivalence ratio on ignition delay time at $p = 2$ atm. (b) The influence of pressure on ignition time at $\Phi = 1$. Symbol: experimental data. Solid line: simulation results.

positively correlated with the dilution ratio of fuel. The higher the dilution ratio, the lower the absolute concentration of cyclohexene at a fixed equivalence ratio. Hence, the global reaction activity is reduced at high dilution ratio, which leads to a decrease in the reaction rate and an increase in the ignition delay time.

Fig. 3b depicts the effect of the equivalence ratio on the ignition delay time with Ar as the inert gas. It clearly shows that the ignition delay time decreases with the increase in the equivalence ratio. Under the experimental conditions, the concentration of cyclohexene is fixed to 2%. With the decrease of equivalence ratio, the content of Ar decreases, and the concentration of O_2 increases. Therefore, the probability of effective collision between cyclohexene and O_2 increases, and the enhanced global reactivity, leading to the reduction of ignition delay time. In general, the developed model fits the experimental data well in the high temperature region below 1350 K. At higher temperatures (>1350 K), the simulation result of ignition delay time is slower than the corresponding experimental result. This deviation is partly due to the measurement error caused by high temperature experiment of the shock tube.[66] On the other hand, it also shows that the developed model of cyclohexene needs to be further improved. As the temperature increases, reaction R1 becomes the most important consumption channel of cyclohexene, which has been determined in the flux analysis as shown in Fig. 6. As the major decomposition product of cyclohexene, the optimization of 1,3-butadiene combustion mechanism is the key point for further model improvement.

4.2 Sensitivity analysis

In order to determine the key reactions that affect the ignition delay time during combustion, the brute-force sensitivity analysis was carried out with the developed model for cyclohexene. The sensitivity coefficient was calculated using the method proposed by Kumar *et al.*[8] The formula is as follows:

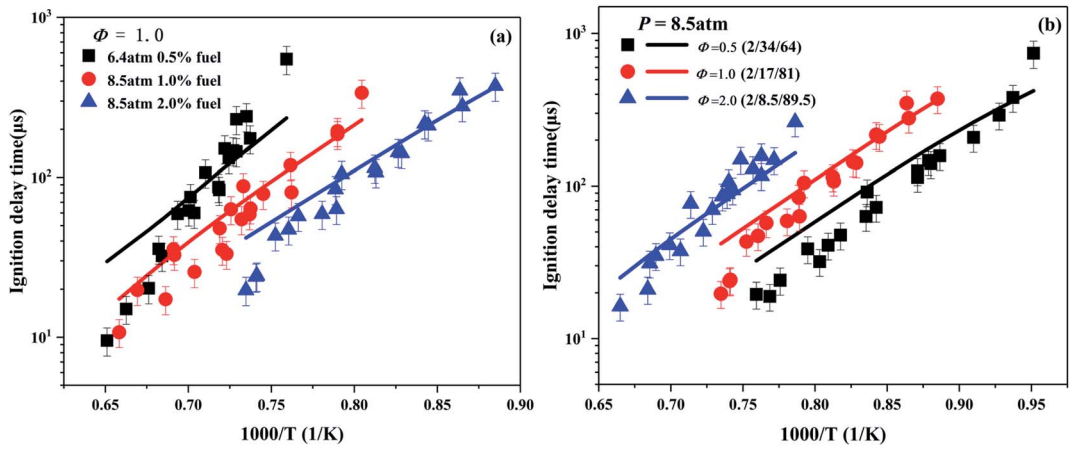

Fig. 3 The ignition delay time of cyclohexene/O_2/Ar mixture. (a) The effect of dilution ratio on ignition delay time at 6.4 atm and 8.5 atm. (b) The effect of equivalence ratio on ignition time. Numbers in the brackets represent the mole percentage of the cyclohexene/O_2/Ar mixture. Symbol: experimental data. Solid line: simulation results.

$$S = \frac{\tau(2k_i) - \tau(k_i)}{\tau(k_i)} \times 100\%$$

where τ is the ignition delay time, k_i is the rate coefficient of the ith reaction, and $2k_i$ indicates increasing k_i by a factor of two. A positive value of S indicates that the corresponding reaction inhibits the reactivity of the ignition process, and *vice versa*.

Fig. 4 shows the sensitivity analysis results of ignition delay at temperatures of 1200 K and 1350 K (p = 2 atm, Φ = 1.0). The reaction of H + O_2 = O + OH is the most critical promotion reaction at both temperatures. It leads to an exponential increase in the number of free radicals, leading to an increase in the global reaction activity. In addition, the H-abstraction reactions of CYHEXEN with O_2 and H are competitive steps. The former is the reaction of two stable species to generate two free radicals, which increases the activity of the reaction, while the latter consumes the free radicals to form resonance-stable CYHEXEN-3J and small molecule, which reduces the reactivity. The reactions of producing vinyl radical (C_2H_3V), C_2H_4 + OH = C_2H_3V + H_2O and C_4H_6 + OH = CH_3CHO + C_2H_3V, also have significant promotion effect. The reason is that the generated C_2H_3V radical react with O_2 quickly by the reaction of C_2H_3V + O_2 = CH_2CHO + O, and generating two free radicals, which increases the activity of the system. Similar to inhibition reaction of CYHEXEN with H, other reactions that consuming active radicals to form stable small molecules also show inhibition effect on the ignition of cyclohexene.

Fig. 5 shows the sensitivity analysis results of ignition delay under different equivalence ratios (p = 2 atm, T = 1200 K). The reactions of H + O_2 = O + OH and CYHEXEN + O_2 = CYHEXEN-3J + HO_2 have significant promotion effect on ignition under equivalence ratios of 0.5–2.0. The former enhances the reactivity of the system by consuming an H atom to generate more active OH radical and O atom, while the latter generates two free radicals by consuming one oxygen molecule, which also promotes the ignition of the system. Besides, when equivalence ratio is 0.5, the sensitivity of H + O_2 = O + OH is extremely high, and the sensitivity decreases with the increase of equivalence ratio, which gives the reason for the crossover of ignition delay time in Fig. 2a. Similar to Fig. 4, the reaction of producing vinyl (C_2H_3V) and the reaction of consuming vinyl have greater promotion of ignition. The reaction related to cyclohexene radical (CYHEXEN-3J), CYHEXEN-3J + O_2 = CYHEXDN13 + HO_2 is a promotion reaction. The main reason is that the produced HO_2 radical promotes the reaction of CH_3 + HO_2 = CH_3O + OH, and the latter has a strong promotion effect on ignition, especially on equivalence ratio of 0.5. Note that the reaction of HO_2 + OH = H_2O + O_2, related to HO_2, has a great inhibition effect. The combination of the above reasons explains the greater promoting effect of CYHEXEN-3J + O_2 = CYHEXDN13 + HO_2 at the equivalence ratio of 2.0 than the equivalence ratio of 0.5 and 1.0. In general, in addition to the hydrogen abstraction reaction of cyclohexene and cyclohexenyl radicals, the reactions of small molecules with O_2, OH, HO_2 and CH_3 also have a greater impact on ignition.

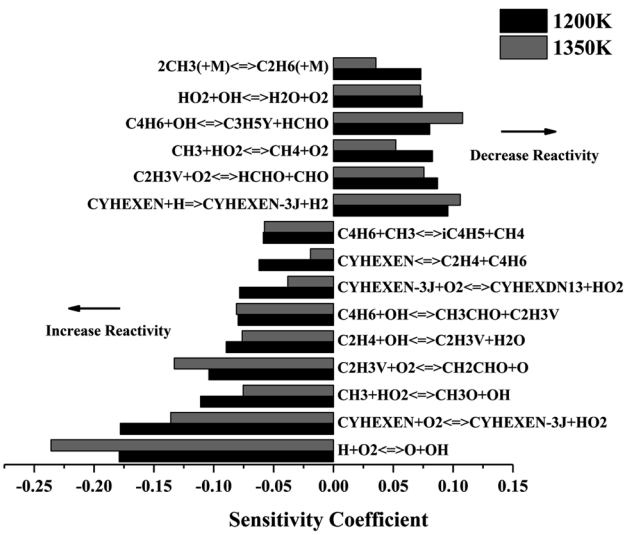

Fig. 4 Sensitivity analysis of cyclohexene–air mixture at different temperatures, and at p = 2 atm, Φ = 1.0.

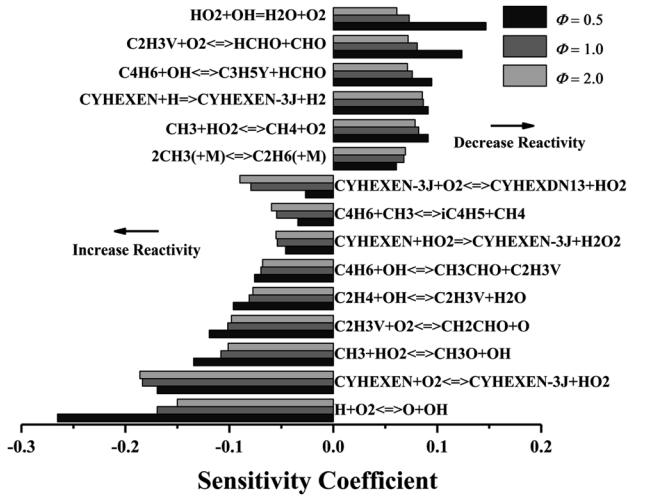

Fig. 5 Sensitivity analysis of cyclohexene–air mixture at different equivalence ratio, and at p = 2 atm, T = 1200 K.

4.3 Flux analysis

The flux analysis of fuel is of great significance for understanding the kinetic process of fuel combustion. The Chemkin-Pro[62] program is used to calculate the contribution of different reactions to the generation or consumption of each species at 20% fuel consumption.

Fig. 6 shows the flux analysis results under low pressure of 2 atm and two high temperature conditions of 1200 K and 1350 K (Φ = 1.0). With the increase of temperature, the proportion of ethylene and 1,3-butadiene generated by the Retro-Diels–Alder reaction of R1 increases from 32.5% to 71.9%, which shows that this reaction becomes the most important consumption channel of cyclohexene at low pressure and high temperature.

This illustrates the importance of further study the mechanism of 1,3-butadiene. As can be seen from Fig. 6, totally 43.8% of cyclohexene generates cyclohexenyl radicals (3-cyclohexenyl

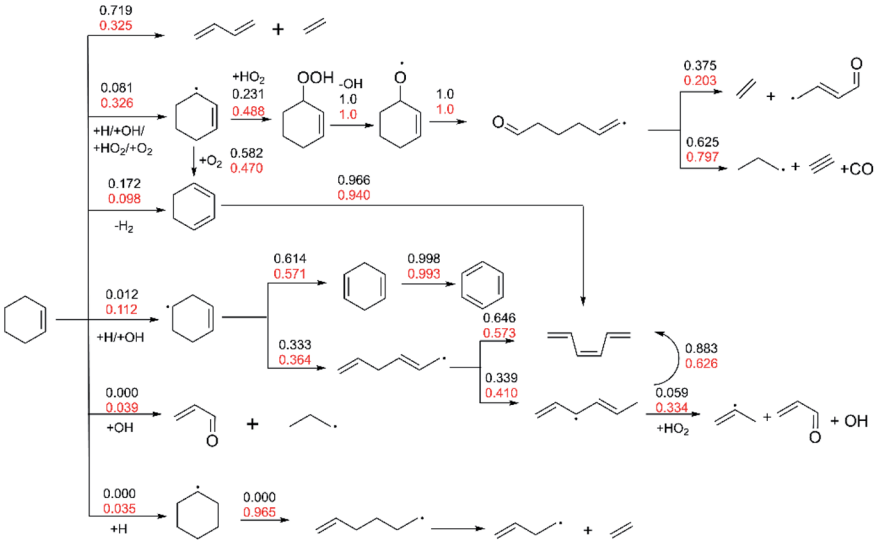

Fig. 6 The flux analysis of 20% cyclohexene consumption under $p = 2$ atm, $\Phi = 1.0$, and high temperature of 1200 K (red number) and 1350 K (black number).

and 4-cyclohexenyl) by the H-abstraction reactions at 1200 K, and the extracted radicals are mainly H atom, OH radical and O_2 molecule. The proportion of 3-cyclohexenyl radical is greater than that of 4-cyclohexenyl radical, which is consistent with the strength of cracking C–H bond in cyclohexene. Previous study[67] shows that the C–H bond energy of allyl position is less than that of the alkyl position. In addition, small proportion of cyclohexene generate 1,3-cyclohexadiene by dehydrogenation reaction and unsaturated enaldehyde through OH addition reaction with the proportion of 9.8% and 3.9%, respectively. On the consumption of cyclohexenyl radicals at 1200 K, 48.8% of 3-cyclohexenyl is converted to hydroperoxides by HO_2 addition reaction, and small molecules are formed through the subsequent bond breaking and ring opening reactions. The remaining 3-cyclohexenyl accounting for 47.0% is consumed by H-abstraction *via* O_2 with the formation of 1,3-cyclohexadiene. Most of the 1,3-cyclohexadiene with the proportion of 94% is isomerized into *cis*-1,3,5-hexatriene. On the other hand, 57.1% of 4-cyclohexenyl strips hydrogen atom to form 1,4-cyclohexadiene, and almost all of 1,4-cyclohexadiene is dehydrogenated to form benzene. The rest of the 4-cyclohexenyl accounting for 36.4% is ring-opened with the formation of hexadienyl radical, which finally converts to *cis*-1,3,5-hexatriene by hydrogen elimination and isomerization reaction. Then, *cis*-1,3,5-hexatriene is eventually converted to small molecules through isomerization, H-abstraction, bond breaking and other reactions. As the temperature increased to 1350 K, the proportion of H-abstraction reaction of cyclohexene decrease greatly, especially the reaction of generating 4-cyclohexenyl almost no longer occurs. The addition reaction of cyclohexene with OH and H no longer happens as well. On the contrary, the ratio of dehydrogenation reaction of cyclohexene to form 1,3-cyclohexadiene is increased to 17.2%. The trend is in accordance with the Le Chatelier's principle. With the fixed pressure and equivalence ratio, the reaction proceeds in the direction of endotherm as the temperature increase. Thus, higher temperature leads to an increased proportion of the endothermic bond breaking reaction of cyclohexene. In addition, Fig. S2† shows the results of flux analysis when the conversion rate of cyclohexene reaches 80%. Compared with the above 20% conversion rate, the difference lies in that the main consumption channel of cyclohexene becomes to the H-abstraction reaction. With the consumption of cyclohexene, the rate of retro-Diels–Alder reaction is reduced due to the decrease of the reactant concentration. On the other hand, the concentration of active free radicals (H, OH and HO_2) increases, and the H-abstraction reaction becomes dominant on the consumption of cyclohexene.

Fig. 7 presents the flux analysis results under pressure of 10 atm and wide temperature range of 770–1200 K ($\Phi = 1.0$). Compared with the results in Fig. 6, the proportion of reaction R1 is greatly reduced with the increase of pressure, accounting for 10.1% at the high temperature of 1200 K. In the whole temperature range, cyclohexene mainly reacts with small molecule of O_2 and free radicals of H and OH to generate cyclohexenyl radicals (3-cyclohexenyl and 4-cyclohexenyl). At medium and low temperature, the proportion of cyclohexene addition reaction with OH increases with the generation of small radicals and unsaturated aldehydes. The corresponding ratios reach 24.1% and 7.4% at the temperature of 770 K. On the consumption of 3-cyclohexenyl, the dominant channel is its addition reaction with HO_2 in the whole temperature range. Another competing channel is the formation of 1,3-cyclohexadiene through the H-abstraction reaction of 3-cyclohexenyl. At high temperature of 1200 K, 1,3-cyclohexadiene is mainly converted into *cis*-1,3,5-hexatriene through isomerization reaction. While at medium and low temperature, it mainly produces benzene through continuous dehydrogenation. Three competing channels are obtained for the consumption of 4-cyclohexenyl. Its dehydrogenation reaction with the formation

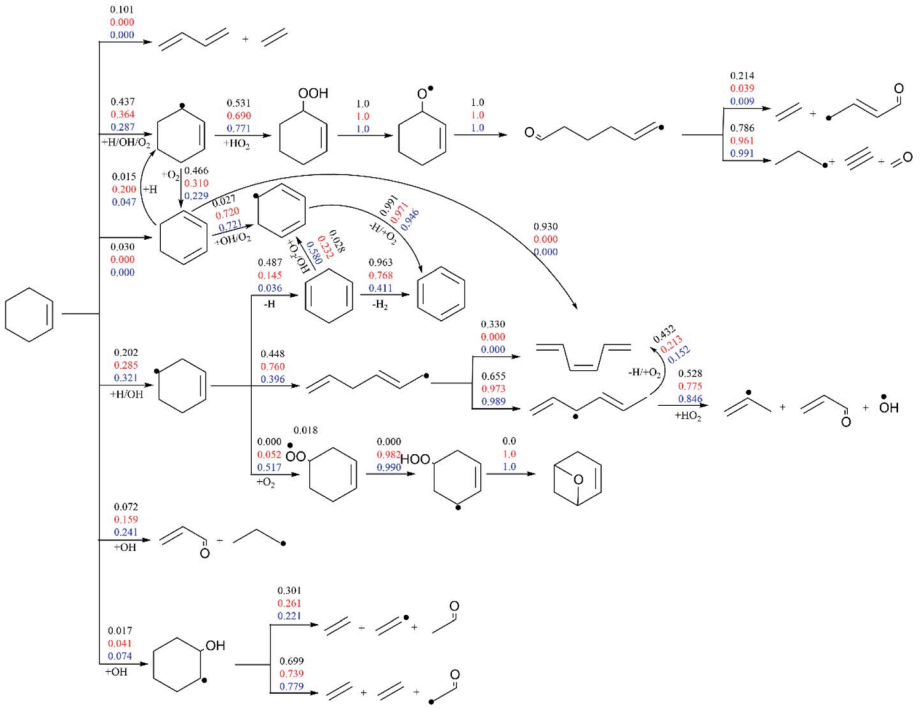

Fig. 7 The flux analysis of 20% cyclohexene consumption under $p = 10$ atm, $\Phi = 1.0$ and temperature of 770 K (blue number), 950 K (red number) and 1200 K (black number).

of 1,4-cyclohexadiene accounts for a larger proportion at high temperature of 1200 K. And then benzene is generated through the successive dehydrogenation of 1,4-cyclohexadiene. The second consumption channel is the ring-opening reaction of 4-cyclohexenyl, which is dominant at the medium temperature. The generated hexadienyl is converted to small molecules finally through isomerization and HO_2 addition reactions. The third channel, 4-cyclohexenyl addition with O_2 to form peroxy radical, only dominants at low temperature. The peroxy radical mainly generates cyclic ether by 1,5 H-shift and O–O bond breaking reactions.

5. Conclusion

This study presents systematic shock tube measurements of ignition delay times for cyclohexene–air mixtures over a wide range of temperature (770–1360 K), pressure (2 atm and 10 atm), and equivalence ratio (0.5, 1.0 and 2.0). By adding high temperature reactions, such as single molecular decomposition, H-abstraction and addition reaction of cyclohexene, to the low temperature mechanism of 1,3-cyclohexadiene, a detailed model is developed to describe the ignition behaviour of cyclohexene. The model shows a good performance on ignition delay times over a wide temperature range in air. However, over predictions are found in Ar-diluted conditions. The sensitivity analyses are carried out to determine the dominant reactions controlling ignition reactivity under different temperatures (1200 K and 1350 K) and equivalence ratios (0.5, 1.0 and 2.0). The reactions of small molecules with O_2, OH, OH_2 and CH_3 in the core mechanism and the H-abstraction reactions of cyclohexene and cyclohexenyl show great influence on ignition. Furthermore, the reactions of $H + O_2 = O + OH$ and CYHEXEN + O_2 = CYHEXEN-3J + HO_2 can be used to explain the change of ignition delay time of cyclohexene with equivalence ratios. Flux analysis gives the change of main reaction pathways under wide temperatures and different pressures. Under the low pressure of 2 atm, when the temperature increases to 1350 K, the retro-Diels–Alder reaction becomes the most important consumption channel of cyclohexene with the proportion of 71.9%. Meanwhile, the ratio of dehydrogenation reaction of cyclohexene to form 1,3-cyclohexadiene is increased to 17.2%. The trend is in accordance with the Le Chatelier's principle. Under the high pressure of 10 atm, the retro-Diels–Alder reaction and the dehydrogenation reaction of cyclohexene to form 1,3-cyclohexadiene are greatly suppressed, and the H-abstraction reaction of cyclohexene with H atom, OH radical and O_2 molecule becomes the main consumption channel of cyclohexene. The model developed in this work provides a better understanding for the combustion chemistry of cyclohexene.

Conflicts of interest

There are no conflicts to declare.

Acknowledgements

The authors gratefully acknowledge the support from National Natural Science Foundation of China (No. 91741201).

References

1 S. M. Burke, U. Burke, R. Mc Donagh, O. Mathieu, I. Osorio, C. Keesee, A. Morones, E. L. Petersen, W. J. Wang, T. A. DeVerter, M. A. Oehlschlaeger, B. Rhodes, R. K. Hanson, D. F. Davidson, B. W. Weber, C. J. Sung, J. Santner, Y. G. Ju, F. M. Haas, F. L. Dryer, E. N. Volkov, E. J. K. Nilsson, A. A. Konnov, M. Alrefae, F. Khaled, A. Farooq, P. Dirrenberger, P. A. Glaude, F. Battin-Leclerc and H. J. Curran, *Combust. Flame*, 2015, **162**, 296–314.

2 J. T. Moss, A. M. Berkowitz, M. A. Oehlschlaeger, J. Biet, V. Warth, P.-A. Glaude and F. Battin-Leclerc, *J. Phys. Chem. A*, 2008, **112**, 10843–10855.

3 C. C. Cao, Y. Zhang, X. Y. Zhang, J. B. Zou, F. Qi, Y. Y. Li and J. Z. Yang, *Fuel*, 2019, **257**, 116039.

4 H. Q. Feng, X. F. Meng, G. Cheng and M. Y. Wang, *Chin. Sci. Bull.*, 2013, **58**, 1072–1078.

5 G. Kukkadapu, K. Kumar, C. J. Sung, M. Mehl and W. J. Pitz, *Proc. Combust. Inst.*, 2013, **34**, 345–352.

6 T. Carriere, P. R. Westmoreland, A. Kazakov, Y. S. Stein and F. L. Dryer, *Proc. Combust. Inst.*, 2002, **29**, 1257–1266.

7 M. M. Kopp, N. S. Donato, E. L. Petersen, W. K. Metcalfe, S. M. Burke and H. J. Curran, *J. Propul. Power*, 2014, **30**, 790–798.

8 K. Kumar, G. Mittal, C.-J. Sung and C. K. Law, *Combust. Flame*, 2008, **153**, 343–354.

9 S. Saxena, M. S. P. Kahandawala and S. S. Sidhu, *Combust. Flame*, 2011, **158**, 1019–1031.

10 Z. J. Wan, Z. J. Zheng, Y. J. Wang, D. X. Zhang, P. Li and C. H. Zhang, *Combust. Sci. Technol.*, 2020, **192**, 2297–2305.

11 S. M. Burke, W. Metcalfe, O. Herbinet, F. Battin-Leclerc, F. M. Haas, J. Santner, F. L. Dryer and H. J. Curran, *Combust. Flame*, 2014, **161**, 2765–2784.

12 Z. W. Qin, H. X. Yang and W. C. Gardiner, *Combust. Flame*, 2001, **124**, 246–254.

13 A. Ramalingam, S. Panigrahy, Y. Fenard, H. Curran and K. A. Heufer, *Combust. Flame*, 2021, **223**, 361–375.

14 Y. J. Zhang, J. H. Cai, L. Zhao, J. Z. Yang, H. F. Jin, Z. J. Cheng, Y. Y. Li, L. D. Zhang and F. Qi, *Combust. Flame*, 2012, **159**, 905–917.

15 Y. Fenard, P. Dagaut, G. Dayma, F. Halter and F. Foucher, *Proc. Combust. Inst.*, 2015, **35**, 317–324.

16 L. Pan, E. J. Hu, J. X. Zhang, Z. M. Tian, X. T. Li and Z. H. Huang, *Fuel*, 2015, **157**, 21–27.

17 Y. Cheng, E. J. Hu, F. Q. Deng, F. Y. Yang, Y. J. Zhang, C. L. Tang and Z. H. Huang, *Fuel*, 2016, **172**, 263–272.

18 M. Ribaucour, R. Minetti and L. R. Sochet, *Twenty-Seventh Symposium (International) on Combustion*, 1998, vol. 1 and 2, pp. 345–351.

19 M. Yahyaoui, N. Djebaili-Chaumeix, C. E. Paillard, S. Touchard, R. Fournet, P. A. Glaude and F. Battin-Leclerc, *Proc. Combust. Inst.*, 2005, **30**, 1137–1145.

20 F. Y. Yang, F. Q. Deng, P. Zhang, E. J. Hu, Y. Cheng and Z. H. Huang, *Energy Fuels*, 2016, **30**, 5130–5137.

21 X. Z. Meng, A. Rodriguez, O. Herbinet, T. Y. Wang and F. Battin-Leclerc, *Combust. Flame*, 2017, **181**, 283–299.

22 H. Wang, Z. Liu, S. Gong, Y. Liu, L. Wang, X. Zhang and G. Liu, *Combust. Flame*, 2020, **212**, 189–204.

23 B. J. Zhong and Z. M. Zeng, *Fuel*, 2020, **278**, 118382.

24 Z. Wang, Z. Cheng, W. Yuan, J. Cai, L. Zhang, F. Zhang, F. Qi and J. Wang, *Combust. Flame*, 2012, **159**, 2243–2253.

25 Z. D. Wang, L. Zhao, Y. Wang, H. T. Bian, L. D. Zhang, F. Zhang, Y. Y. Li, S. M. Sarathy and F. Qi, *Combust. Flame*, 2015, **162**, 2873–2892.

26 J. X. Wang, W. Y. Sun, G. Q. Wang, X. Y. Fan, Y. Y. Lee, C. K. Law, F. Qi and B. Yang, *Proc. Combust. Inst.*, 2019, **37**, 1091–1098.

27 N. Hansen, T. Kasper, B. Yang, T. A. Cool, W. Li, P. R. Westmoreland, P. Osswald and K. Kohse-Hoinghaus, *Proc. Combust. Inst.*, 2011, **33**, 585–592.

28 O. Lemaire, M. Ribaucour, M. Carlier and R. Minetti, *Combust. Flame*, 2001, **127**, 1971–1980.

29 G. Dayma, P. A. Glaude, R. Fournet and F. Battin-Leclerc, *Int. J. Chem. Kinet.*, 2003, **35**, 273–285.

30 L. Giarracca, F. Isufaj, J. C. Lizardo-Huerta, R. Fournet, P. A. Glaude and B. Sirjean, *Proc. Combust. Inst.*, 2021, **38**, 1017–1024.

31 Z. K. Hong, K. Y. Lam, D. F. Davidson and R. K. Hanson, *Combust. Flame*, 2011, **158**, 1456–1468.

32 M. Ribaucour, O. Lemaire and R. Minetti, *Proc. Combust. Inst.*, 2002, **29**, 1303–1310.

33 W. J. Li, M. E. Law, P. R. Westmoreland, T. Kasper, N. Hansen and K. Kohse-Hoinghaus, *Combust. Flame*, 2011, **158**, 2077–2089.

34 L. Chen, T. L. Zhang, C. Y. Li, W. N. Wang, J. Lu and W. L. Wang, *Comput. Theor. Chem.*, 2013, **1026**, 38–45.

35 P. Dagaut, A. Ristori, A. Frassoldati, T. Faravelli, G. Dayma and E. Ranzi, *Proc. Combust. Inst.*, 2013, **34**, 289–296.

36 H. Wang, E. Dames, B. Sirjean, D. A. Sheen, R. Tango, A. Violi, J. Y. W. Lai, F. N. Egolfopoulos, D. F. Davidson, R. K. Hanson, C. T. Bowman, C. K. Law, W. Tsang, N. P. Cernansky, D. L. Miller, R. P. Lindstedt, A high-temperature chemical kinetic model of n-alkane (up to n-dodecane), cyclohexane, and methyl-, ethyl-, n-propyl and n-butyl-cyclohexane oxidation at high temperatures, *JetSurF version 2.0*, September 19, 2010, http://web.stanford.edu/group/haiwanglab/JetSurF/JetSurF2.0/index.html.

37 A. Schönborn, M. D. Le, R. Fournet, P. A. Glaude, V. Warth and B. Sirjean, *Combust. Flame*, 2019, **205**, 466–483.

38 F. Battin-Leclerc, *Prog. Energy Combust. Sci.*, 2008, **34**, 440–498.

39 J. Zádor, C. A. Taatjes and R. X. Fernandes, *Prog. Energy Combust. Sci.*, 2011, **37**, 371–421.

40 K. L. Yong, J. N. He, W. F. Zhang, L. Y. Xian, C. H. Zhang, P. Li and X. Y. Li, *Fuel*, 2017, **188**, 567–574.

41 C. H. Zhang, B. Li, F. Rao, P. Li and X. Y. Li, *Proc. Combust. Inst.*, 2015, **35**, 3151–3158.

42 J. N. He, Y. D. Gou, P. F. Lu, C. H. Zhang, P. Li and X. Y. Li, *Combust. Flame*, 2018, **192**, 358–368.

43 M. Yang, Z. J. Wan, N. X. Tan, C. H. Zhang, J. B. Wang and X. Y. Li, *Combust. Flame*, 2020, **221**, 20–40.

44 L. Shi, D. D. Chen, Z. J. Zheng, P. Xu, R. Wang and C. H. Zhang, *Combust. Flame*, 2021, **232**, 111540.

45 H. K. Ciezki and G. Adomeit, *Combust. Flame*, 1993, **93**, 421–433.
46 K. A. Heufer and H. Olivier, *Shock Waves*, 2010, **20**, 307–316.
47 E. L. Petersen, M. Lamnaouer, J. de Vries, H. Curran, J. Simmie, M. Fikri, C. Schulz and G. Bourque, *Discrepancies between shock tube and rapid compression machine ignition at low temperatures and high pressures*, Berlin, Heidelberg, 2009.
48 E. L. Petersen, *Combust. Sci. Technol.*, 2009, **181**, 1123–1144.
49 D. Darcy, H. Nakamura, C. J. Tobin, M. Mehl, W. K. Metcalfe, W. J. Pitz, C. K. Westbrook and H. J. Curran, *Combust. Flame*, 2014, **161**, 65–74.
50 M. Chaos and F. L. Dryer, *Int. J. Chem. Kinet.*, 2010, **42**, 143–150.
51 G. A. Pang, D. F. Davidson and R. K. Hanson, *Proc. Combust. Inst.*, 2009, **32**, 181–188.
52 Z. M. Tian, Y. J. Zhang, L. Pan, J. X. Zhang, F. Y. Yang, X. Jiang and Z. H. Huang, *Energy Fuels*, 2014, **28**, 5505–5514.
53 R. Fournet, J. C. Bauge and F. Battin-Leclerc, *Int. J. Chem. Kinet.*, 1999, **31**, 361–379.
54 B. Sirjean, R. Fournet, P. A. Glaude, F. Battin-Leclerc, W. J. Wang and M. A. Oehlschlaeger, *J. Phys. Chem. A*, 2013, **117**, 1371–1392.
55 J. Zádor, S. J. Klippenstein and J. A. Miller, *J. Phys. Chem. A*, 2011, **115**, 10218–10225.
56 C. W. Zhou, Y. Li, U. Burke, C. Banyon, K. P. Somers, S. T. Ding, S. Khan, J. W. Hargis, T. Sikes, O. Mathieu, E. L. Petersen, M. AlAbbad, A. Farooq, Y. S. Pan, Y. J. Zhang, Z. H. Huang, J. Lopez, Z. Loparo, S. S. Vasu and H. J. Curran, *Combust. Flame*, 2018, **197**, 423–438.
57 Z. Serinyel, O. Herbinet, O. Frottier, P. Dirrenberger, V. Warth, P. A. Glaude and F. Battin-Leclerc, *Combust. Flame*, 2013, **160**, 2319–2332.
58 Z. D. Wang, L. L. Ye, W. H. Yuan, L. D. Zhang, Y. Z. Wang, Z. J. Cheng, F. Zhang and F. Qi, *Combust. Flame*, 2014, **161**, 84–100.
59 M. R. Zeng, Y. Y. Li, W. H. Yuan, T. Y. Li, Y. Z. Wang, Z. Y. Zhou, L. D. Zhang and F. Qi, *Proc. Combust. Inst.*, 2017, **36**, 1193–1202.
60 C. W. Gao, J. W. Allen, W. H. Green and R. H. West, *Comput. Phys. Commun.*, 2016, **203**, 212–225.
61 Y. C. Chang, M. Jia, Y. D. Liu, Y. P. Li and M. Z. Xie, *Combust. Flame*, 2013, **160**, 1315–1332.
62 *CHEMKIN-PRO 15112, Reaction Design*, San Diego, 2011.
63 Y. Li, C. W. Zhou and H. J. Curran, *Combust. Flame*, 2017, **181**, 198–213.
64 R. X. Fernandes, K. Luther and J. Troe, *J. Phys. Chem. A*, 2006, **110**, 4442–4449.
65 J. Troe, *Combust. Flame*, 2011, **158**, 594–601.
66 V. P. Zhukov, V. A. Sechenov and A. Y. Starikovskii, *Combust. Flame*, 2008, **153**, 130–136.
67 A. L. Koritzke, J. C. Davis, R. L. Caravan, M. G. Christianson, D. L. Osborn, C. A. Taatjes and B. Rotavera, *Proc. Combust. Inst.*, 2019, **37**, 323–335.